Received: 2 December 2021 | Revised: 2 March 2022 | Accepted: 8 April 2022

IET Intelligent Transport Systems

DOI: 10.1049/itr2.12195

The Institution of Engineering and Technology WILEY

ORIGINAL RESEARCH

Autonomous vehicles' intended cooperative motion planning for unprotected turning at intersections

Donghao Zhou[1,2] | **Zian Ma**[1,2] | **Xiaohui Zhang**[1,2] | **Jian Sun**[1,2]

[1]The Key Laboratory of Road and Traffic Engineering, Ministry of Education, Tongji University, Shanghai, China

[2]The Department of Traffic Engineering, Tongji University, Shanghai, China

Correspondence
Jian Sun, Department of Traffic Engineering, Tongji University, Cao'an Road, No. 4800, Shanghai 201804, China.
Email: sunjian@tongji.edu.cn

Funding information
National Key Research and Development Program of China, Grant/Award Number: 2018YFB1600505; National Natural Science Foundation of China, Grant/Award Number: 52125208

Abstract

Turning behaviour is one of the most challenging driving manoeuvres that take place at intersections. Autonomous vehicles (AVs) are often overly conservative in these scenarios as they compromised to others' behaviour to realize behavioural consistency. This paper proposes an intended cooperative motion planning (ICMP) that can actively predict the intentions of interacting participants. This helps achieve socially compliant cooperation and enables each vehicle to converge upon a set of consistent behaviours. The ICMP framework divides the integrated driving process into two related modules: prediction and planning. These modules are integrated using the mechanism of intended cooperation, which first introduces the criteria for a cooperative response and then maps them in the motion planning space. The prediction module applies a Gaussian mixture model to learn human drivers' behaviour to determine conflict points, which helps to narrow down the solution spaces. In the planning module, paths are represented by quartic Bézier curves and speed is modelled as a polynomial function. Optimizations can then be used that maximize the efficiency and smoothness for path planning, and comfort and efficiency for speed planning. The test results show that ICMP-based AVs had consistent interactions with other vehicles. Moreover, when compared with a potential field-based method, the ICMP-based method had better performance in terms of safety, comfort and efficiency, especially when interacting with multiple oncoming vehicles.

1 | INTRODUCTION

INTERSECTIONS account for 40% of driving accidents and represent a critical issue in the urban transportation system [1]. The main concern is when the autonomous vehicles (AV) make unprotected left turns at intersections they have to interact with multiple oncoming manually driving vehicles (MVs), as Figure 1 shows the typical scenario. Previous studies have demonstrated the complexity of driving in these situations, with some characteristics such as limited priority [2] and variation in trajectories [3]. In these multi-interaction environments, even the self-driving cars of Waymo, which are some of the most advanced in the field of AV, become excessively conservative in unprotected turning situations [4, 5]. These overly conservative behaviours are not only underproductive in terms of AVs' efficiency, but may also annoy other drivers and lead to road rages, deadlock and traffic accidents [6].

The key issue of these multi-interaction systems is realizing behavioural consistency under uncertainties. In the past few decades, some approaches have claimed that the future traffic environments are predictable [7–9]. Thus, AVs can predict the future intentions or movements of participants and plan in a way that is consistent with others. However, multiple factors can simultaneously influence future states, and these factors cannot be comprehensively extracted and represented. As such, deviations in prediction are inevitable and uncertainties still exist. Other approaches have tried to model the interaction process based on theoretical methods like game theory [10], the Markov decision process (MDP) [11] and its extensions [12]. The major challenge these approaches face is the curse of dimensionality. Since traffic environments are unstructured, the number of objects is changeable and their movement parameters (such as position and speed) are continuous. Discretization of the space of observation and action states is difficult because the number

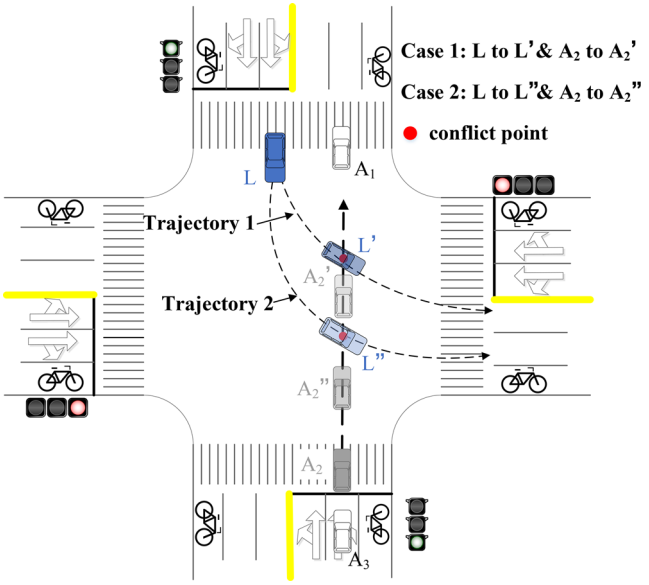

FIGURE 1 A typical unprotected turn scenario where the behaviours of the turning vehicle and the oncoming vehicle are interrelated

of interacting agents is not fixed and high-dimensional spaces exponentially increase the computational cost. Since uncertainties in prediction or modelling have not been tackled properly in previous studies, AVs have to compromise to their interacting participant for safety which may lead to some overly conservatively behaviours.

In this paper, we tried to reduce the uncertainty involved in intention prediction by creating planning that considers other vehicles' reaction. This allows us to lead each participant to converge with consistent behaviour. This idea was inspired by the process of behavioural convergence, where interacting participants could gradually adjust their motion and observe the other's reactions until their behaviours converge to the same result. Using this process, some empirical criteria can be extracted. By instilling these criteria in motion planning, this paper proposed intended cooperative motion planning (ICMP). The ICMP enables AVs to consider the oncoming vehicle's reactions and therefore to realize the behavioural consistency. When the oncoming vehicle does not want to yield, the AV would obey its higher priority and yield. When the oncoming vehicle is willing to share its right-of-way, the AV would try to preempt.

However, several challenges are inevitable while implementing ICMP. First, the motion planning of turning vehicle is influenced by dynamic factors like the vehicle's state, and the states and the intentions of the oncoming vehicles. As shown in Figure 1, determining the crossing gap (namely determining the interacting vehicle) is challenging because the AV L have to create plans after a comprehensive analysis of all factors like the states and the intentions of all oncoming vehicles A_1 A_2 A_3. Furthermore, the behaviours of participants are interdependent. When L tends to move along trajectory 2 (*L* to "L"), A_2 may preempt and move to A_2'. However, if L would like to preempt and move to L', L must have confidence that A_2 would yield to L and move to A_2 rather than insisting on preemptive decision and moving to A_2' causing a sever conflict. The turning vehicle's planning has to consider its influence on other participants in case arising adverse effects on the interacting participants like deviating from the behavioural consistency. In addition, the interrelated plan and prediction make it hard to do a cooperative decision. For example, when L moves along trajectory 2 (L to L") after predicting A_2 would preempt (A_2 to A_2'), A_2 may misunderstand the intention of L and moves to L, which leads to temporary deadlock. How to enable AV to understand MVs behaviour and behave understandably to other MVs, namely achieve socially compliant driving [13], is of great challenge. Last, but not the least, as the planning has an effect on the decision, simultaneous decision-making and planning may rely on iterative convergence, which can significantly increase computational costs.

To tackle these challenges, the complex motion planning process was decomposed into prediction and planning modules. The main contributions of this work are summarized as follows:

1. We designed a prediction-planning integrated framework that enables AVs to actively considers others' intentions to achieve overall consistency. The framework consists of intention recognition, conflict points prediction, and optimization-based path and speed planning.
2. We analyzed the mechanism of intended cooperation. Criteria for cooperative responses were proposed. By mapping the criteria to the turning vehicle's motion planning space, a cooperative motion planning space was extracted, which ensures that the motion planning solution in the extracted space leads to the cooperative response of interacting participants. This helps search a socially compliant cooperative motion plan.
3. We developed a Gaussian mixture model to learn human drivers' preference to determining conflict points, which helped narrow down the feasible region of motion planning and contribute to the diversity of the AVs' trajectories.

The rest of this paper is organized as follows. Section 2 presents a literature review of the existing motion planning studies. Section 3 introduces the ICMP in detail. A case study is conducted in Section 4 and the simulation results are analyzed in Section 5. Finally, Section 6 presents a conclusion and a direction for future studies.

2 | LITERATURE REVIEW

Motion planning at intersections involves multiple associated problems like prediction, decision making and trajectory planning that have been widely studied. Depending on how the interactions are modelled, three types of planning methods can be implemented: trajectory prediction-based, intention-aware planning and joint planning of multiple participants.

The trajectory prediction-based approaches assume that the future states of participants are determined and predictable.

They directly predict trajectories of other participants while ignoring their intentions and treat the prediction result as constraints for the AVs' planning. Some methods assume some kinematic parameters are constant and use kinematic theory to predict the trajectories of other participants [14, 15]. However, some studies have shown that motion is usually uncertain because of measurement error and stochastic behaviour. Researchers have applied Gaussian regression and Kalman Filters to reduce the uncertainties. Deep learning approaches are also regarded as helpful in behaviour modelling and prediction [16] in non-linear systems. However, it remains to be seen if neural networks developed in one situation can be applicable to other situations [17].

Instead of simply predicting trajectories, the intention-aware approaches pay more attention to higher-level concepts like intention recognition and decision-making. They distinguish different driving intentions and then create plans that consider different characteristics in various situations. The mainstream approaches include rule-based, game theory and probability-based approaches.

Rule-based approaches try to simulate the motion of participants with explicit functions or classifiers, such as the logit model [18] or decision-tree model. However, rigid rules cannot ensure the robustness of motion planning in different contexts. To tackle this problem, some studies have proposed hierarchical frameworks that integrate multiple tasks and behaviour patterns for different situations [19–21]. Finite state machines (FSM) have also been used, as they integrate many rules for driving in different contexts. The efficiency of FSMs has been proven in the DARPA Grand Challenge [22, 23]. However, this method still lacks the ability to generalize to unknown situations and deal with uncertainties.

Game theory has been used for decision-making to account for the interactions between vehicles. For example, a non-cooperative Nash game was used to estimate a counterpart's intention in response to the subject vehicle's intention [24]. Besides, a Stackberg Game was formulated to achieve more realistic decision-making of human behaviour and therefore incorporate the underlying decision-making mechanism of human drivers into AVs' motion planning [25]. However, the game assumed that each participant perfectly knew the intention space and payoff function of other participants, which may lead to aggressive and potentially dangerous behaviour owing to overconfidence in the behaviour model.

The probability-based approaches treat the multi-interaction issue as a process of probability-based state transition, where intentions may be visible or hidden. The reliability of a certain situation in the future was evaluated based on a hidden Markov model (HMM) or Bayesian inference [9]. For example, a framework based on a hybrid-state system was developed to model driver behaviour near intersections, where HMMs were then trained to estimate driver behaviour from filtered continuous observations [26]. The method was tested and showed better performance than a K-Nearest Neighbor (KNN) approach. However, the interactions between vehicles were neglected, which means that some interrelated intentions like crossing, yielding, lane changing and car following were ignored. In [27], a transfer deep reinforcement learning (RL) framework was constructed, where the decision-making policy learned from one driving task at an intersection was transferred in another driving mission. However, the studied scenario was simple where few participants were involved. Also, the data for training and evaluation were both from simulations. In [28], a long short-term memory (LSTM)-based network was employed to encode vehicle historical motion features, the graph attention network (GAT) and a synthesized network were integrated to model vehicle–vehicle interaction and vehicle–motorcycle interaction.

While trajectory-based and intention-aware approaches focus on the behaviour of individuals, joint planning methods highlight the inner-relations among participants. The most typical methods are MDP and its extensions like the partially observed MDP (POMDP). For example, in [29], a critical turning point-based hierarchical planning approach was proposed that included a high-level candidate path generator and a low-level POMDP-based planner. POMDP was also applied to realize motion planning with interactions and uncertain intention predictions in [30]. In [31], the critical turning points were first to generate turning path while the POMDP served as a speed profile solver. The limitations of POMDPs remain in terms of poor computational efficiency and their generality for arbitrary traffic conditions. In [32, 33], the state transitions of interacting agents were modelled by a hierarchical dynamic Bayesian network (DBN), while the decisions of all participants were made by continuous POMDPs. However, this approach did not account for the complexity caused by mixed flow intersections, and few interacting agents existed at these intersections.

In summary, the existing studies have the following limitations. First of all, they typically examine traffic conditions where the number of interacting participants is fixed, which may not be applicable to multiple interaction scenarios. Since a participant's actions are interdependent of all others' actions, multiple interactions would exponentially increase uncertainty and result in the freezing robot problem [34]. Furthermore, although intention-aware and joint planning approaches can try to realize overall behavioural consistency at the intention level, most of them just follow others' intentions, which may lead to overly conservative behaviours. How to enable AV to seek cooperation and behave understandably to other MVs, namely achieve cooperation [13], is to be settled. To the best of the authors' knowledge, no existing processes can handle the complexity of multiple interactions at interactions on a reasonable scale, let alone realizing socially compliant cooperation in these scenarios.

3 | METHODOLOGY

3.1 | Problem statement

An illustration of interactive motion planning is shown in Figure 2. The majority of human drivers do not always act

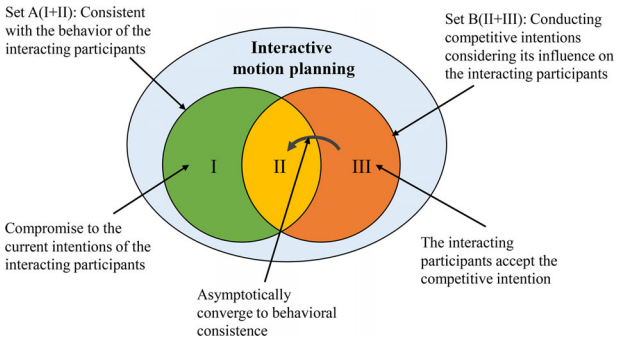

FIGURE 2 Different categories while conducting interactive motion planning

consistently, especially when encountering improper behaviour. Strictly following others' intentions may result in conservative behaviour (in Area I). On the other hand, some subject vehicles may have competitive intentions that influence other interacting participants. An interacting participant may accept the competitive intention on a reasonable scale (in Area III) and cooperate with the subject vehicle by slowing down. Through cooperation, the interacting participants may adopt a response such that their behaviours can converge. This is represented by the arrow pointing from Area III to Area II. Hence, learning and performing motion planning is a basic way to actively communicate with other traffic participants.

An AV's motion planning P_L involves influential factors like the vehicle's own state S_L and the state and intention of interacting participants S_A and M_A . This relationship is represented by the motion planning function f_{MP} in Equation (1). Furthermore, the intentions of the interacting participant are adaptive: the interacting participants can adjust their own intentions according to the AV's planning P_L and its state S_A to realize behavioural consistency. Some rules and representative factors, like the cooperative acceleration a_c (please see Section 3.3 for more details), can be deduced to determine the intentions under the influence of the AV, as represented by Equation (2).

$$P_L = f_{MP}(S_L, S_A, M_A) \tag{1}$$

$$M_A = f_Y(P_L, S_A) = f_Y(a_c) \tag{2}$$

Therefore, AVs can actively make plans that consider the response of the interacting participant to realize the cooperation. This paper proposes ICMP methods that can generate necessary cooperative responses from the interacting participant. We first developed the criteria for recognizing a cooperative response by determining the movements that would cause an interacting participant to behave in a certain way. Then, we mapped the rules to the motion planning space to consider the potential responses of the interacting participants. Thus, a larger solution space became available, where interacting participants' potential reactions were considered, as shown in Figure 3. This way helps produce cooperative planning solutions while searching in the extended space.

This paper focused on the decision and planning layers of AVs and the perception is not our focal point. We assume all vehicles' states (i.e. position, speed, heading, acceleration) are perfectly known.

3.2 | Framework

Multiple prediction-planning frameworks are usually sequentially based [35–37]. In these frameworks, AVs first predict the intentions or trajectories of interacting agents, then make a motion planning based on the prediction results. However, sequential schemes ignore the fact that other vehicles' motion may be influenced by the AVs' motion. A proper prediction-planning scheme should include a closed-loop mechanism where AV can influence the prediction and the prediction provides feedback for motion planning [38]. This paper proposes a prediction-planning integrated framework that enables AVs to actively predict the response of interacting participants. The integrated prediction-planning task was decomposed into two highly related modules: prediction and planning, as presented in Figure 4.

The two modules were integrated using the mechanism of intended cooperation. First of all, the criteria for recognizing cooperative response were established. Furthermore, by mapping the criteria to the motion planning space, a cooperative motion planning space was extracted. The cooperative motion planning space can guarantee that each motion plan in the space would elicit a cooperative response from the interacting participant. The ICMP claims were developed to illustrate the mapping. Please see Section 3.3 for additional details.

In the prediction module, AVs first predict the potential conflict points. Conflict points are not only a critical input for determining a cooperative response, but also an important factor for narrowing down the search space for motion planning. After determining the conflict points, some path and speed planning can be conducted in the planning module. Given the planning result, the AV can determine if the interacting participant would yield for overall consistency based on the ICMP claims.

In the planning module, we first determine the region of the cooperation indicator (within the cooperation time range T_p) to represent the cooperative motion planning space. Then, we implement some methods to perform path and speed planning in the cooperative motion planning space. In the case of the path planning, an optimized Bezier curve was developed. For speed planning, a quartic polynomial speed function was used and optimized for safety and comfort. Please see Section 3.5 for more details.

After generating trajectories given the conflict points, trajectory drivability and collision-avoidance checkers are set to select feasible and collision-free trajectories. The minimum-cost trajectory within them is the planned trajectory. If there is no such a trajectory that satisfies the constraint, the planned path is deemed irrational. Turning is deemed a high-risk behaviour and the AV adjusts its decision to decelerate instead of insisting on crossing instantly.

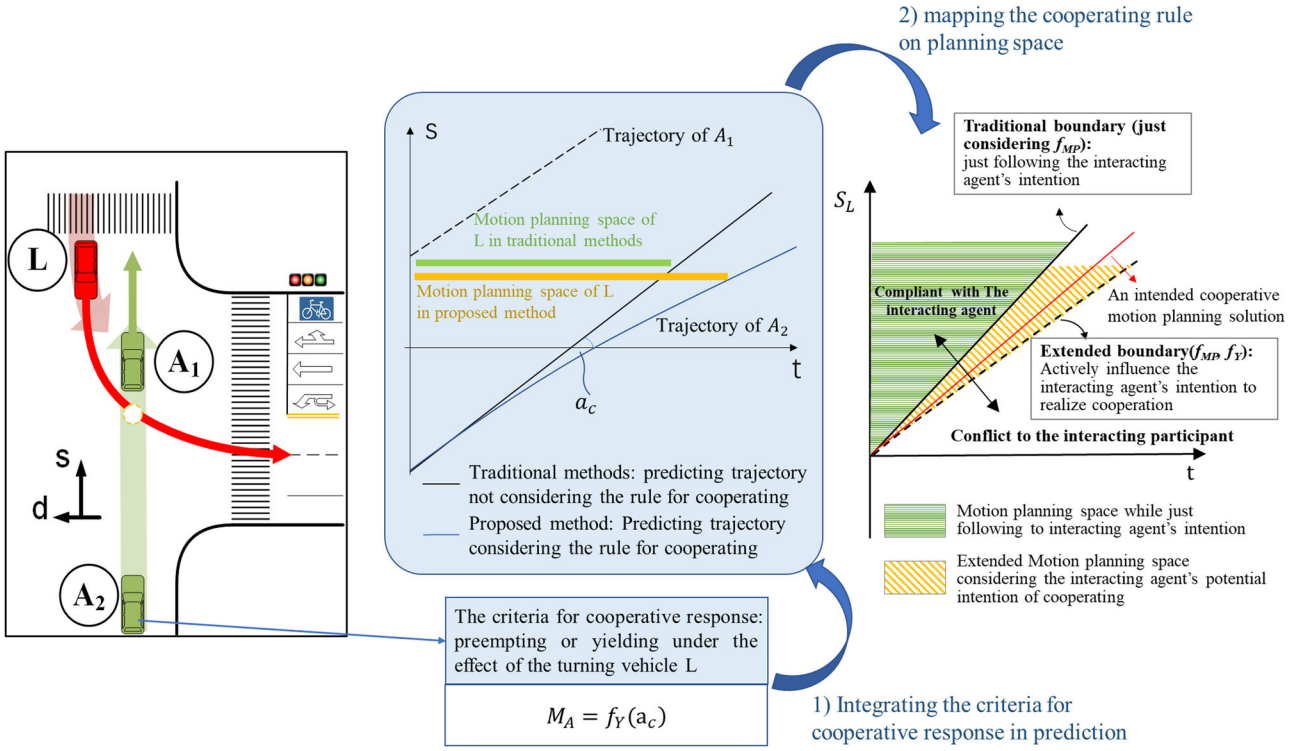

FIGURE 3 Motion planning space extended to consider the interacting agent's response

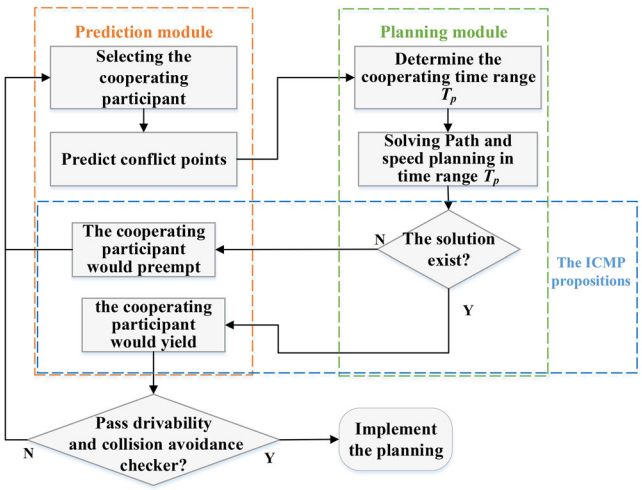

FIGURE 4 A prediction-planning integrated framework for intended cooperative motion planning

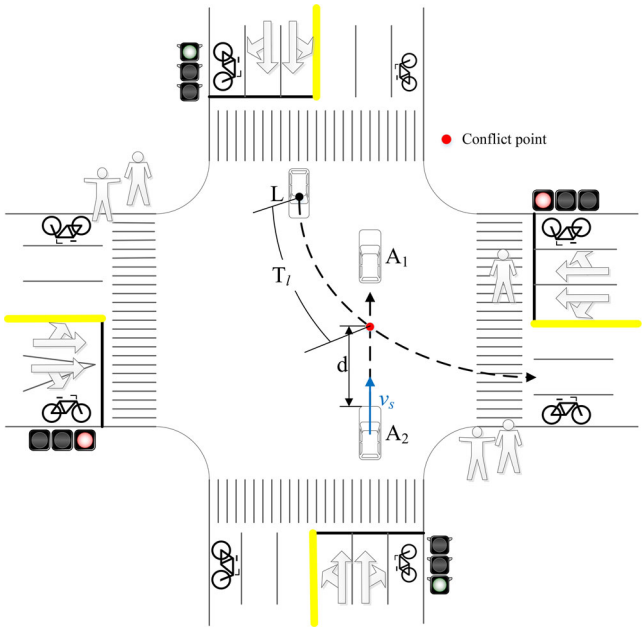

FIGURE 5 Related parameters while determining the cooperative acceleration

3.3 | Mechanism of intended cooperation

3.3.1 | Criteria for a cooperative response

To realize the ICMP, AVs first have to understand how their interacting participants would react to the AVs' motion. Although multiple methods such as HMMs [39], regression [26] and finite-state machines [40] have been applied for intention recognition, few of them have considered the influence of the AVs' motion. This paper utilizes the index, cooperative acceleration, for intention recognition that involves both the state of the interacting participant and the AV.

The cooperative acceleration a_c is defined as the maximum acceleration of the cooperating vehicle A_2 that allows it to avoid a collision with the left-turning vehicle L, as shown in Figure 5. It can reflect the loss of comfort that the turning behaviour may

bring to the interacting road users. In addition, the variable in kinematics reflects the critical acceleration of A_2 that can guarantee A_2 and L arrive at the conflict point at the same time. The cooperative acceleration a_c can be determined by the following equation:

$$a_c = \frac{2\,(d - v_s T_l)}{T_l^2} \tag{3}$$

where T_l is the left-turning vehicle's arrival time at the conflict point, d is the distance between the interacting vehicle and the conflict point, and v_s is the speed of the interacting vehicle.

The cooperative acceleration is related to both the state of the cooperating vehicle (i.e. position and speed) and the AVs' planning (i.e. arrival time at the conflict point). This parameter is an anticipated measurement that indicates the loss of the comfort of A_2. From a qualitatively perspective, when the cooperative acceleration is large, A_2 has to accelerate sharply if vehicle A_2 wants to arrives the conflict point slightly after vehicle L. To avoid this unnecessary comfort loss and to ensure safety, vehicle A_2 tends to yield to vehicle L. On the contrary, when the cooperative acceleration is small, A_2 has to decelerate significantly if vehicle A_2 wants to pass the conflict slight before vehicle L. To avoid this sharp deceleration, vehicle A_2 was likely to preempt. From a quantitative perspective, according to the decision tree constructed in [19], we have recognized there was a threshold of cooperative acceleration H that can be used for recognizing the intention of the interacting vehicle. Empirical evidences on the assumption and calibration of this threshold are presented in Section 4.2.

3.3.2 | ICMP claims

Based on the cooperative acceleration-based criteria for intention recognition, AVs are capable of recognizing how the interacting agents would make decisions and can react to their motion. However, AVs have to move in a way that ensures the AVs' intentions remain consistent with that of the interacting vehicle. The AVs should turn when the interacting agents are willing to yield, and the AVs should yield when the interacting agents want to continue on their path. Two claims were proposed to realize this by mapping the cooperative acceleration-based criteria to the time range of motion planning. The proof of two claims is introduced in the Appendix.

Claim 1. If there exists a feasible motion plan for the AV that can ensure that it would arrive at the conflict point within the cooperation time range T_p , the cooperating agent is willing to yield to the AV, and the AV can preempt.

Claim 2. If there exists no feasible motion plan to make sure that the AV arrives at the conflict point within the cooperation time range T_p , the cooperating agent would preempt and the AV should yield to the cooperating agent.

The cooperating time range T_p in the claims refers to the time the cooperating vehicle takes to arrive at the conflict point given the acceleration value threshold H. T_p can be found using the following equation:

$$v_s T_p + \frac{1}{2} H\, T_p^{\,2} = d \tag{4}$$

$$T_p = \begin{cases} x_1, \text{ if } H > 0 \\ x_2, \text{ if } -\dfrac{v_s^{\,2}}{2d} < H < 0 \\ M, \text{ if } H < -\dfrac{v_s^{\,2}}{2d} \end{cases} \tag{5}$$

The solutions of Equation (4) include three conditions, which are shown in Equation (5). When $H < -\frac{v_s^{\,2}}{2d}$, there are no real solutions to the equation. This condition means that the speed of the interacting vehicle would decelerate to zero before it arrives at the conflict point. In this case, T_p can be regarded as a large number M. When $H > -\frac{v_s^{\,2}}{2d}$, there are two real solutions to the equation: x_1 and x_2 . We assume x_1 is the smaller one and x_2 is the larger one. When $-\frac{v_s^{\,2}}{2d} < H < 0$, we know that $x_1 > 0$ and $x_2 > 0$. This condition represents the cooperating vehicle decelerates but its speed would not drop to zero when it arrives at the conflict point. T_p is equal to the smaller value x_1 . When $H > 0$, we see $x_1 < 0$ and $x_2 > 0$. This condition means that the cooperating vehicle would accelerate towards the conflict point. T_p is equal to the positive value x_2 .

The two claims reflect the intentions of the cooperating agents and how they are influenced by the states of themselves and AVs' planning simultaneously. On the other hand, the two claims indicate that if an AV would preempt the conflict point, the AV must make a feasible plan that falls within the cooperation time range such that the interacting participant would cooperate with it. The claims enable AVs to make motion plans and recognize the interacting agent's intentions without iterative feedback for intention recognition and motion planning.

3.4 | Prediction module

The prediction module predicts the manoeuvre of the interacting vehicle given the time to the conflict point t_c based on the proposed interaction mechanism. The planning module then searches a feasible value that considers the vehicle A_2 is willing to yield. To determine the time to the conflict point, we first determine the position of the conflict point. However, the position of the conflict point varies greatly because the conflict

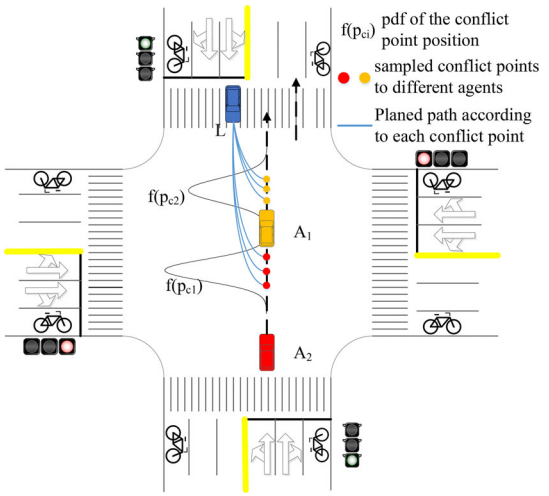

FIGURE 6 Learning human-like preferences for determining and sampling conflict points

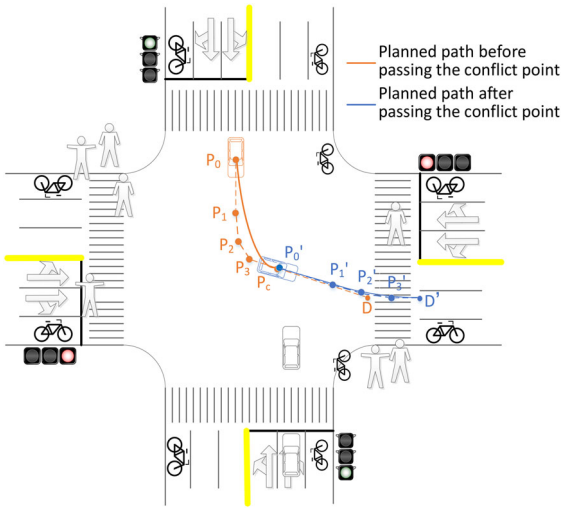

FIGURE 7 Path planning before (yellow lines) and after passing the conflict point based on Bézier curves

points adapt to deal with different interactions. AVs have to consider a variety of conflict point distributions.

One method that can be used to predict conflict points is sampling all possible points in the conflict area. This approach usually leads to large computational costs. To solve this, previous studies have proposed a concept of learning human-driving behaviour for AV planning [32, 41]. Using this, we propose a method that learns human preferences for determining conflict points. The human preferences were modelled using probability distribution functions drawn from the empirical MVs driving data. AVs can sample conflict points according to the PDF, as shown in Figure 6.

A Gaussian mixture model (GMM) was then used to model these human preferences for conflict points. GMMs are a probabilistic model used to represent normally distributed subpopulations within an overall population. They have been widely used in clustering, state prediction [42], and so on. GMMs do not require knowing which subpopulation a data point belongs to, allowing the model to learn the subpopulations automatically.

First, two types of behaviours for oncoming vehicles were classified. The first type considered the behaviour of the leading vehicle of the vehicle sequence. Since the leading vehicle is only influenced by the left-turning vehicle, the input vector for the GMM only involves terms for the leading and the left-turning vehicles. The second type considers the behaviour of the following vehicles. The following vehicle interacts with both the left-turning and the proceeding vehicles. Therefore, the input vector includes terms for themselves, the left-turning and the proceeding vehicles.

As such, we constructed two types of GMMs to model the different behaviours. For the leading vehicle, we defined the five-dimensional input vector as $I = [v_l, h_l, \Delta x, \Delta y, v_s]'$, where v_l is the speed of the AV, h_l is the heading of the AV, Δx_l, Δy_l are latitude and longitude positional differences between the AV and the interacting agent, and v_s is the speed of the interacting agent. For the following vehicles, we defined their input vector as $I = [v_l, h_l, \Delta x, \Delta y, v_s, d_f, v_f]'$, where d_f is the distance between the following vehicle and its proceeding vehicle, and v_f is the speed of the proceeding vehicle. The parameters are showed in Figure 6.

The output vector $O = [d]$, where v_l is the speed of the AV, h_l is the heading of the AV, Δx, Δy are positional differences between the AV and the interacting agent, and v_s is the speed of the interacting agent. We generated states $G = [I, O]'$ that describe the relation between a given situation I and the output O. We assumed that the distribution of G could be approximated with a finite Gaussian mixture distribution:

$$G \sim \sum_{k=1}^{n} \omega_k N(\mu_k, \Sigma_k) \tag{6}$$

where ω_k is the weight, $\mu_k \in \mathbb{R}^n$ is the mean, and $\Sigma_k \in \mathbb{R}^n$ is the covariance matrix of the kth Gaussian distribution. n is the total number of Gaussian models in the mixture.

Then we trained the Gaussian mixture distribution using empirical data. Based on the trained Gaussian mixture distribution, we were able to predict the distribution of the output vector O given certain values of elements in the input vector I. The output vector O follows a new Gaussian mixture distribution. The following equations help extract the new Gaussian mixture distribution of output vector O.

First, we sorted the dimensions of the mean vectors and covariance matrices according to whether they were part of the input parameters or the output parameters

$$\mu_k = \left[\mu_{k,i}, \mu_{k,o}\right] \tag{7}$$

$$\Sigma_k = \begin{bmatrix} \Sigma_{k,i} & \Sigma_{k,i,o} \\ \Sigma_{k,o,i} & \Sigma_{k,o} \end{bmatrix} \tag{8}$$

where i denotes the index of the input-dimensions and o denotes the index of the output-dimensions. The covariance matrix of the conditional output is calculated by

$$\Sigma_{(k,o|i)} = \Sigma_{k,o} - \Sigma_{k,o,i}\Sigma_{k,i}^{-1}\Sigma_{k,i,o} \tag{9}$$

The output mean of each component can be computed by

$$\mu_{(k,o|i)} = \mu_{k,o} + \Sigma_{k,o,i}\Sigma_{k,i}^{-1}\left(I - \mu_{k,i}\right) \tag{10}$$

The influence of each component is computed by

$$\omega_{k|i} = \frac{\omega_k p\left(I|N\left(\mu_k, \Sigma_k\right)\right)}{\sum_{k=1}^{n} \omega_k (I|N\left(\mu_k, \Sigma_k\right)} \tag{11}$$

Finally, the conflict points can be sampled for the Gaussian mixture distribution of the output vector.

3.5 | Planning module

3.5.1 | Path planning

The path planner tried to generate a feasible path given the initial states of the AV and the conflict point. Bézier curves were applied here to generate the local paths, which can easily guarantee smoothness and continuity. Since the computational cost increased with the degree of the Bézier curve, a lower degree was preferable. A quartic Bézier curve was sufficient for satisfying the requirements of curvature boundaries and continuity [43]. Figure 7 shows the planned Curve l before the AV arrives at the conflict point. P_0 represents the position of the AV, and P_c is the conflict point. P_1 , P_2 , P_3 are control points of the quartic Bézier curve. D is the destination where the AV leaves the intersection. The direction from P_0 to P_1 is consistent with the AV's heading. P_3 , P_c and D are collinear.

The parametric equation is

$$B\ (\tau) = \sum_{k=0}^{4} C_4^k\, P_k (1-\tau)^{4-k} \tag{12}$$

Since the position of the AV (P_0), the AV's heading and the position of the conflict point were available, the position of control points were crucial for generating the curve. The positions of control points were determined by optimizing the curve.

$$\begin{aligned}(P_1, P_2, P_3) &= \arg\min_{P_1,P_2,P_3} \int_l B' + B'' + B'''\, ds \\ &= \arg\min_{P_1,P_2,P_3} \int_0^1 B'(\tau) + B''(\tau) + B'''(\tau)\, d\tau\end{aligned} \tag{13}$$

The objective function of the optimization involved terms of the first, second, and third-order derivatives of the curve parametric equation, which aimed to minimize the speed, acceleration, and jerk for higher efficiency and better smoothness.

After the AV crosses the conflict point, the AV can adjust its speed and heading to ensure that its heading is consistent with the road heading when it leaves the intersection as shown in Figure 7.

3.5.2 | Speed planning

Speed planner tried to plan how the AV moves along the planned path. Since calculating integration and derivative function of polynomials is easy so the function of position, speed, and acceleration can be conveniently transferred. A polynomial function $s(t)$ was developed to model AV's position, where t is time, and s is the distance to the origin along the path. As pointed out in [44], the optimal control trajectory can theoretically optimize the speed change (minimize the time integral of the squared jerk) by ensuring that the sixth derivative of the positional function is equal to 0.

$$\frac{d^6 s}{dt^6} = 0 \tag{14}$$

Therefore, we denoted the position function $s(t)$ as a quintic polynomial

$$s(t) = a_0 + a_1 t + a_2 t^2 + a_3 t^3 + a_4 t^4 + a_5 t^5 \tag{15}$$

The coefficients $a_i (i = 1, 2, \ldots, 5)$ were determined by the following optimization:

$$\min f = \alpha W_1 \left(\int_0^{T_e} s'''(t)\, dt \right) + (1-\alpha)\, W_2\, (T_e) \tag{16.a}$$

s.t.

$$s(0) = 0 \tag{16.b}$$

$$s'(0) = v_{l,t0} \tag{16.c}$$

$$s''(0) = a_{l,t0} \tag{16.d}$$

$$s(T_e) = L_p \tag{16.e}$$

$$v_{\min} \le s'(t) \le v_{\max},\ t \in [0, T_e] \tag{16.f}$$

$$a_{\min} \le s''(t) \le a_{\max},\ t \in [0, T_e] \tag{16.g}$$

$$jerk_{\min} \le s'''(t) \le jerk_{\max},\ t \in [0, T_e] \tag{16.h}$$

$$T_f \le T_e \le T_p \tag{16.i}$$

where T_e is the time the AV spends driving along the planned path. $W_1(\cdot)$ *and* $W_2(\cdot)$ are min–max normalization functions. α is a weight to adjust the bias of the optimization, where this paper used a balanced weight, namely $\alpha = 0.5$. $v_{l,t0}$, $a_{l,t0}$ are the speed and acceleration of the AV at the planning moment t_0. L_p is the length of the planned path. v_{min} and v_{max} are the upper and lower bounds of the AV's speed. a_{min} and a_{max} are the upper and lower bounds of accelerations. $jerk_{min}$ and $jerk_{max}$ are the upper and lower bounds of jerks. The object of optimization considered both efficiency and comfort. Equations (16.b)–(16.e) represent some given state information at the start or end points. Equations (16.f)–(16.h) try to constrain the value of speed, acceleration, and jerk. Equation (16.i) applies the claims that time range of motion planning should be less than T_p to preempt the conflict point. T_f is the expected arrival time to the conflict point of the oncoming vehicle before the crossing gap. This constraint is removed after the AV passes the conflict point.

3.5.3 | Trajectory dynamics-awareness and collision avoidance constraints

After the path and speed planning, the kinematic trajectory should be converted into the dynamics-aware trajectory to better control the vehicle. The quintic polynomial-based speed profile can be transferred to dynamic control parameters as pointed out in [43]. A tracking error serving as a re-planning indicator was also proposed in [43] which indicated regenerating a planning if the tracking error was larger than a threshold. In this paper, however, we real time update the planning so the tracking error is not necessary. Instead, drivability checks [44] are integrated into the speed planning process

$$\min J\left(S(t_2), \hat{S}(t_2; S(t_1), u)\right) \tag{17}$$

where $S(t_2)$ is the planned state at t_2 and $\hat{S}(t_2; S(t_1), u)$ is vehicle's state at t_2 given the kinematic model initial state $S(t_1)$ and the input vector u. J denotes the position and orientation error between two states. If the errors for all adjacent states in the planned trajectory are smaller than a recommended threshold, the trajectory can pass the drivability checker. Otherwise, the trajectory is infeasible.

Due to some MVs maynot move as the AV excepts, the collision avoidance constraints were proposed for security. For AV, attention should be placed on moments of insecurity, which are crucial for evaluating safety performance. The collision-avoidance constraint is presented:

$$TTC_{m_0}^{k} \geq TTC_{min}, \ \forall k \in K \tag{18}$$

Equation (18) means for each planned trajectory m_0, we can calculate the TTC value at each time interval k, namely ($TTC_{m_0}^{k}$), within the time range K. All these TTCs should be larger than a minimal TTC threshold TTC_{min} in case high-risk conflicts.

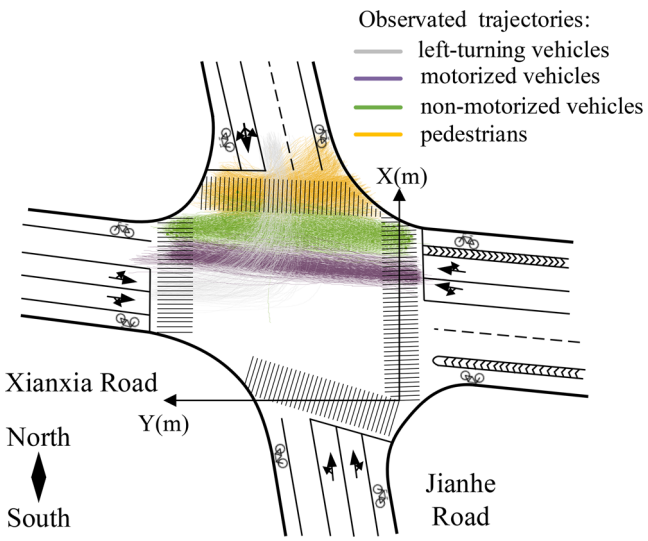

FIGURE 8 The observed trajectories at the Jianhe-Xianxia intersection

The real-time feedback was set from the trajectory drivability and collision-avoidance checker to AV's decision. If there was no such a trajectory that can pass the drivability checker and satisfy the constraint, the planned path was deemed irrational. The AV would select the next oncoming vehicle as its cooperating object and repeat the forehead steps again. If all these oncoming vehicles were not willing to yield to the AV, turning was deemed a high-risk behaviour. The AV would adjust its decision to decelerate and wait another gap to cross instead of insisting on crossing instantly.

4 | CASE STUDY

4.1 | Study site and data collection

Since the proposed model was designed to handle the complexity of turning AV motion planning, a mixed-flow intersection with frequent vehicular interaction is suitable. Left-turn behaviour is more difficult to simulate than right turn. Therefore, left-turning vehicles at the Jianhe-Xianxia intersection in Shanghai were studied, which is a typical two-phase intersection.

The empirical trajectory data of left-turn vehicles were extracted from a video recorded with high accuracy video-processing software. The video recorded traffic operations during rush hours from 4:00 PM to 5:40 PM. The observed trajectories are shown in Figure 8. Among the 210 left-turn trajectories, 141 left-turn vehicles interacted with motorized oncoming vehicles while other left-turn vehicles merely interacted with non-motorized vehicles. The trajectories of these 141 left-turn vehicles were studied.

4.2 | Parameter calibration

The criteria for cooperative response were calibrated according to empirical data. In a previous work [19], we calibrated a

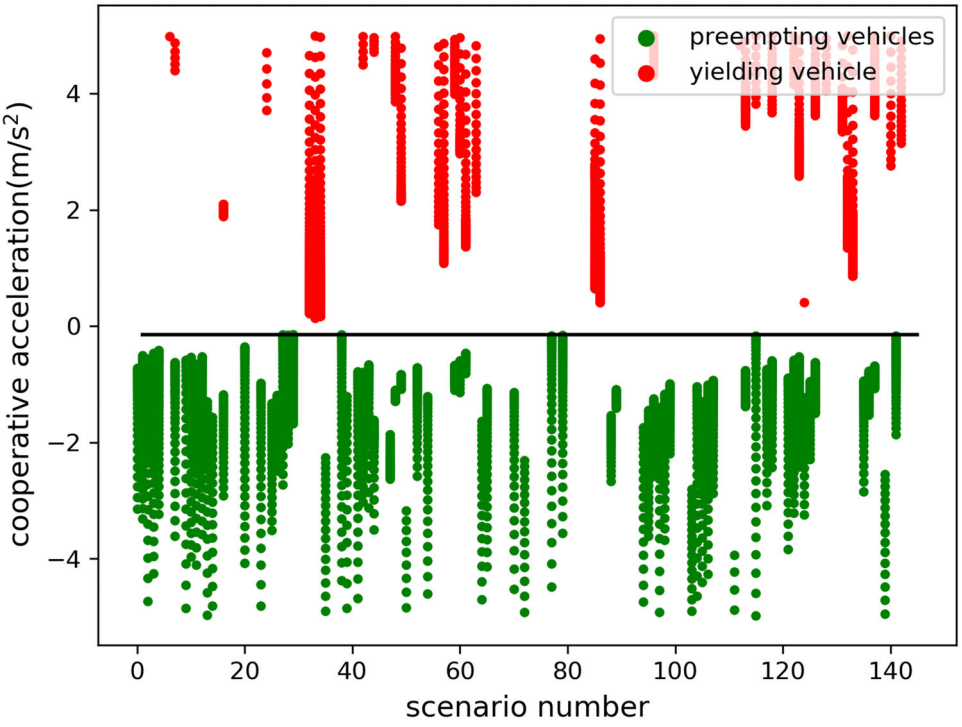

FIGURE 9 Cooperative acceleration of the opposite-going vehicles in each

decision tree for the turning criteria, which can also be used to model the intention of the interacting vehicle: preempting or yielding. The decision tree in [19] involved two terms: the cooperative acceleration and the delay if yielding. Based on the decision tree, the cooperative acceleration threshold H was valued as $-0.15\,\mathrm{m/s^2}$, and the delay threshold was valued as 3.39 s. When the cooperative acceleration was greater than $-0.15\,\mathrm{m/s^2}$, the interacting vehicle would yield, and the left turning vehicle would preempt. When the collaboration acceleration was less than $-0.15\,\mathrm{m/s^2}$, the delay caused by yielding will be considered. If the delay was greater than 3.39 s, the interactive vehicle would preempt because of the loss of too much time, and the left turning vehicle would yield. If the yield delay was less than 3.39 s, the interactive vehicle would choose to yield and the turning vehicle would go first.

Although the criteria can accurately simulate the limited priority phenomenon, in the field of AV, we tend to assume that AVs will obey the traffic rules more than human beings in the same situation to ensure safety. Therefore, this paper assumed that when the collaborative acceleration was less than $-0.15\,\mathrm{m/s^2}$, the left-turning AV would adopt the yield intention without considering the delay. However, a problem occurred that if the delay was more than 3.39 s, both the left-turning AV and the interacting vehicle would yield to each other. Although a stalemate may appear, it avoids the dangerous condition where both sides think they can preempt. In addition, for the two vehicles' different behaviour of yielding, this stalemate will be broken as the vehicles move on.

Figure 9 shows the cooperative accelerations of the oncoming vehicles in each scenario. The oncoming vehicles were

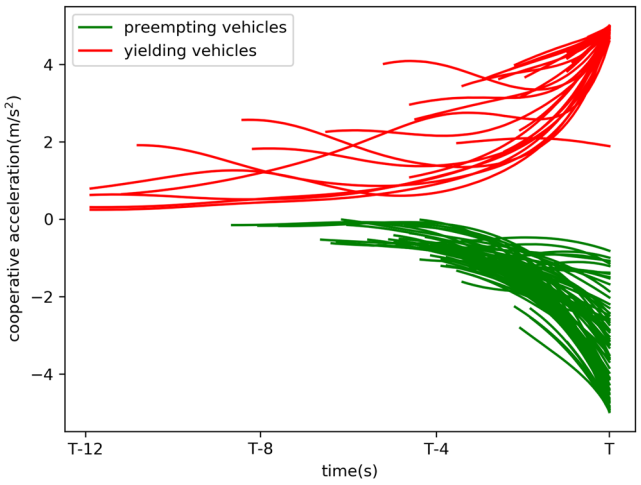

FIGURE 10 Cooperative accelerations of each yielding vehicle before they arrive at the conflict point. T is the time that the preempting vehicle arrives at the conflict point

divided into two classes: The opposing vehicles whose cooperative accelerations were larger than H and were willing to yield and those whose cooperative acceleration was less than H and tended to preempt. This revealed that the cooperative acceleration could indicate the oncoming vehicles intention. Cooperative accelerations of yielding vehicles tended to be larger than the threshold H, while cooperative accelerations of not-yielding vehicles were less than the threshold H.

Furthermore, Figure 10 shows the cooperative accelerations of each yielding vehicle before their arrival at the conflict point.

By comparing their cooperative accelerations with the threshold H, we found that oncoming vehicles' intentions were continuous before arriving to the conflict point. Therefore, threshold H with a value of $-0.15\,\mathrm{m/s^2}$ was reasonable.

5 | TEST RESULTS AND ANALYSIS

To evaluate the effectiveness of the proposed algorithm, a simulation platform was developed. The study site was built in the simulation based on the empirical Xianxia-Jianhe intersection. The initial states of left-turning and oncoming vehicles are same to the empirical trajectory data. However, their subsequent behaviours are controlled by different models. The left-turning vehicles are controlled by the ICMP method, while the behaviours of oncoming vehicles are simulated by intelligent driver model (IDM) [45].

First, the accuracy of intention prediction was studied as it directly indicates if the ICMP result received the cooperative responses from the interacting participants.

Furthermore, two types of motion planning methods: intended cooperation motion planning (ICMP) and a potential field (PF)-based approach proposed in [46] were installed in the AVs and their behaviours were compared for the same scenarios. The PF-based approach was recently published and focused on the same multi-interaction issues in unprotected turning scenarios. The PF-based planning performs well from the aspects of intention recognition and trajectory planning. More importantly, it is unfair for these methods to directly apply them in different study sites and different scenarios. The potential field method was proposed for the same study site with same collected data which would not cause problems of fairness. We reckon it is a more equitable way to compare these two works. The varied behaviours of AVs facing high-density traffic flow were presented.

Finally, a statistical comparison was conducted in terms of post-encroachment time (PET), travel time, and the jerk of AVs. PET can reflect the safety performance when interacting with other vehicles. Compared with the other widely used safety indicator TTC, PET reflects the observed severity of conflict, while TTC is an anticipated risk measurement indicating the time leaving for drivers to avoid collision. Travel time can reflect the efficiency in mobility. Compared with other efficiency indicators like delay and waiting time, travel time can also indicate the mobility at the intersection and does not require the intersection being crowded. Jerk is a fundamental index that indicates the comfort, which is more informative to present the distribution of vehicle's acceleration change and the frequency of sharp acceleration

5.1 | Performance of the intended cooperation

Table 1 shows the confusion matrix of the prediction to the reaction of the interacting participant to evaluate the performance of intended cooperation.

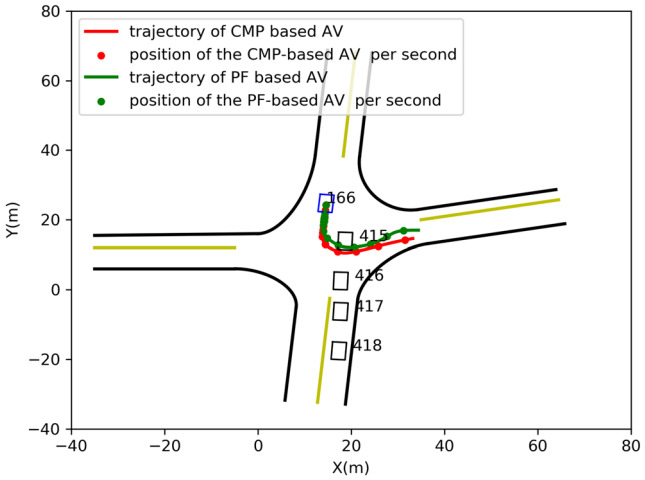

FIGURE 11 Initial positions of participants and trajectories of left-turning AVs based on two methods (Note: Vehicles 419–421 are far away from the intersection at the initial time so they are not presented in the figure)

The accuracy and recall are calculated. The high accuracy and recall showed that the success rate of intended cooperation was high. Besides, when the two vehicles conflicted with each other, the riskiest situation was when the left-turning vehicle expected the interacting vehicle to yield, but actually the interactive vehicle wanted to preempt. In this case, the intentions of the two vehicles were inconsistent, which would cause severe conflicts. Although the high recall rate indicates that these fierce conflicts were occasional, the potential dangers still existed. However, real-time rolling prediction and collision avoidance can effectively avoid these risks.

5.2 | A typical case: crossing high-density traffic flow

The purpose of conducting this case study was to test the ability to cooperate with interacting agents. The high-density traffic flow indicated that gaps between vehicles were small and that the AV needs to seek a potential cooperating participant to cross through. Figure 11 shows the initial states of the participants and trajectories of left-turning AVs based on two methods, when they suffered the same traffic situation.

As shown in Figure 12, three critical moments t_1 , t_2 , and t_3 were found. From 0 to t_1 , the speed of the interacting par-

TABLE 1 Confusion matrix of intention prediction

		Actual	
The reaction of the interacting agent		**Preempting**	**Yielding**
Predicted	Preempting	76	1
	Yielding	3	55

$$Accuracy = \frac{TP}{TP + FN} = 97.04\%$$

$$Recall = \frac{TP+TN}{TP+TN+FP+FN} = 96.20\%$$

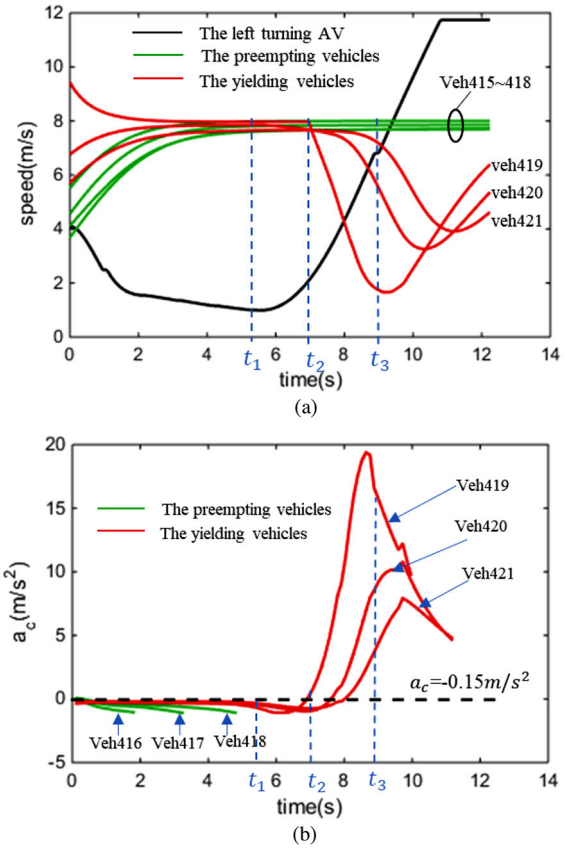

FIGURE 12 The critical parameters that change for the interacting participants in the ICMP-based case. (Note: t_1 is the time when the AV successfully made the cooperative acceleration. t_2 is the time when the cooperative acceleration of the cooperating vehicle (Veh. 419) reaches the threshold. t_3 is the time when the turning AV crossed the conflict point). (a) The cooperative acceleration of the interacting participants in the ICMP-based case. (b) The speed of the interacting participants in the ICMP-based case

ticipants (Veh. 416–421) converged to the desired speed of the IDM, while their cooperative accelerations were approximately equal to the threshold. At t_1 , the AV successfully found a cooperative plan, determined the cooperating agent (Veh. 419), and started to implement its planning. From t_1 to t_2 , although the speed of Veh. 419 was constant, its cooperative acceleration first came down and then rose up because the ICMP-based AV was adjusting its speed to influence it. The cooperative acceleration of Veh. 419 reached the threshold at t_2 , and kept rising, which meant that Veh. 419 was more likely to yield. Then as the AV moved, from t_2 to t_3 Veh. 419 kept slowing down. At t_3 the AV crossed the conflict point so Veh. 419 started to accelerate until it could also leave the intersection.

While the ICMP-based AV crossed sequential vehicles through the gap between Veh. 418 and Veh. 419, the PF-based AV yielded to all the oncoming vehicles in the same scenarios. The gap between Veh. 418 and Veh. 419 was not large enough for the PF-based AV to cross. However, the ICMP-based AV made a plan considering the reaction of Veh. 419 to the planning. Since Veh. 419 would yield and decelerate, the gap would become large enough to cross. Therefore, when compared with the PF-based AV, the ICMP-based AV considered its influence on the other participants and exploited the potential of cooperative interaction with conflict agents. The videos of these two cases were uploaded on this website (Link: https://pan.baidu.com/s/1z6MH_SVYBpm9gYr8IV7L_w, Extraction Code: s6ua).

5.3 | Statistical analysis in safety, efficiency, and comfort

To statistically compare the performances of the ICMP-based AVs and PF-based AVs, we reconstructed the traffic scenarios in simulation according to the empirical data. Two AVs with different motion planning methods were tested in these scenarios. Then, we collected the trajectories of the participants and conducted some statistical analyses in terms of safety, efficiency, and comfort. Three indexes post-encroachment time (PET), travel time, and jerk were determined to reflect the AVs' performances of safety, efficiency, and comfort, respectively. Besides, to explore AVs' performance when suffering different oncoming traffic demands, we divided the left-turning scenarios into three groups according to the traffic demand (low oncoming flow rate: 0—800 veh/h, medium oncoming flow rate: 801–1200 veh/h, high oncoming flow rate: larger than 1200 veh/h). The statistical parameters of the indices, means, standard deviations (SDs), and *p*-value are presented in Table 2.

5.3.1 | Post-encroachment time (PET)

Post-encroachment time (PET) has been used in many previous studies and has been proven suitable for representing the severity of conflict during crossing events [20]. According to a previous study [47], the threshold PET was defined as 8 s, which represents the minimal conflict severity. A PET larger than the threshold PET means that a conflict is too small and can be ignored.

The results of statistical parameters showed that the PETs of ICMP-based AVs were significantly larger than those of PF-based AVs with a 95% confidence level when suffering low and medium oncoming flow. The average PETs of the two AVs also reflected this tendency. However, when suffering high oncoming flow, the PETs of ICMP-based AVs had no significant difference. The reason is that the high oncoming flow made the gaps among the vehicles small so that both AVs had to become more cautious.

As shown in Figure 13, when comparing the PETs of the two AVs scenario by scenario, ICMP-based AVs had better safety performance in 80% of the scenarios no matter which level of oncoming traffic demand they suffered. In addition, ICMP-based AVs created less severe conflicts (PET<1 s) in low and medium oncoming flow rates. The reason was that ICMP-based AVs could precisely predict the intentions of the interacting participants and were able to plan accordingly. As such, the severe conflicts which occurred when both interactive parties wanted to preempt were avoided. In addition, the precise prediction was also able to benefit collision avoidance. When interacting

TABLE 2 Statistical parameters of PET statistical parameters of performance indexes

Oncoming flow rate	AV type	PET (s)			Travel time (s)			Jerk (m/s^3)		
		Mean	SD	*P*-val .	Mean	SD	*P*-val .	Mean	SD	*P*-val .
Low	ICMP	3.86	1.03	0.04	7.49	4.26	0.35	0.03	0.75	0.00
	PF	2.75	1.38		9.42	5.31		-0.07	0.68	
Med.	ICMP	4.56	1.49	0.01	10.57	5.84		0.01	0.64	0.01
	PF	3.37	1.79		11.15	7.75	0.73	0.06	0.68	
High	ICMP	4.06	1.07	0.26	7.13	5.24	0.38	0.05	0.78	0.00
	PF	3.42	1.74		9.13	7.24		0.06	0.68	

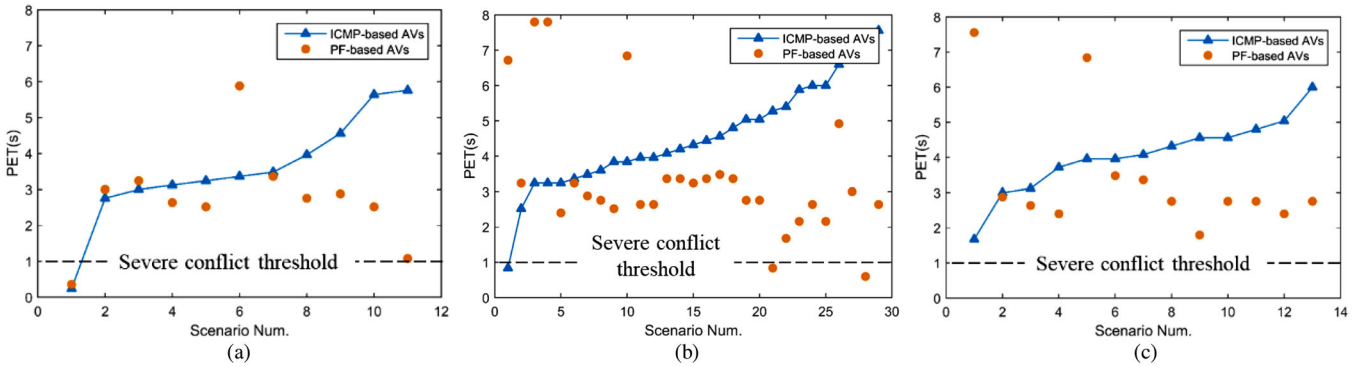

FIGURE 13 PETs of two kinds of AVs with different oncoming flow rates. (a) Low oncoming flow rate; (b) medium oncoming flow rate; (c) high oncoming flow rate

with high-flow-rate oncoming vehicles, there was less room for ICMP-based AVs to achieve cooperation and both two AVs had to be cautious. Although ICMP-based AVs were significantly safer than PF-based AVs, both AVs performed well in terms of safety.

5.3.2 | Travel time

The distributions of the travel times of the ICMP-based AVs and the PF-based AVs are shown in Figure 14. Although the results of the rank-sum test show that there was no significant difference with each oncoming traffic demand level, the average travel time of the ICMP-based AVs was less than the PF-based AVs. The maximum travel time of CMP-based AVs was also less than PF-based AVs. In most cases, significant differences did not exist. However, in some scenarios, PF-based AVs had to yield to all conflicting agents which led to large travel time (larger than 25 s). However, ICMP-based AVs were able to select a gap to cross through, which decreased the travel time. We can claim that ICMP-based AVs were overly efficient. Besides, this figure also indicates that medium-flow-rate oncoming vehicles can provide more cooperative responses. Low-flow-rate oncoming traffic means the difference of whether cooperation or not is not such large and high-flow-rate may provide less opportunities for cooperation.

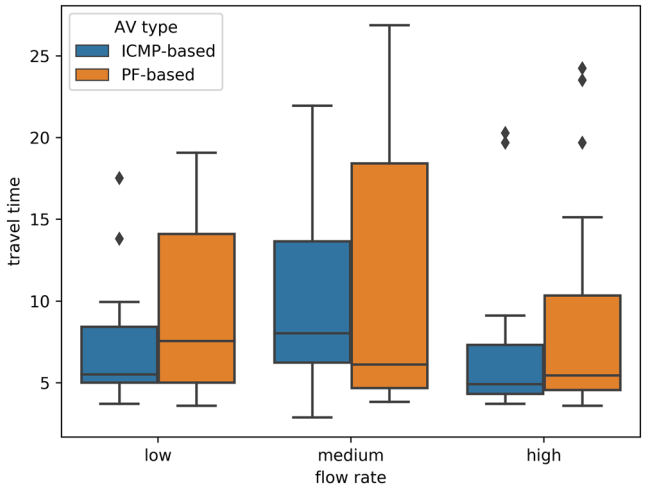

FIGURE 14 Travel time of two kinds of AVs with different oncoming flow rates

5.3.3 | Jerk

Jerk was used to reflect the comfort performance. To analyze the comfort of AVs, the jerks of AVs were collected. As is shown in Figure 15, for both the ICMP-based and PF-based AVs, a large portion of the absolute values of the jerk were less

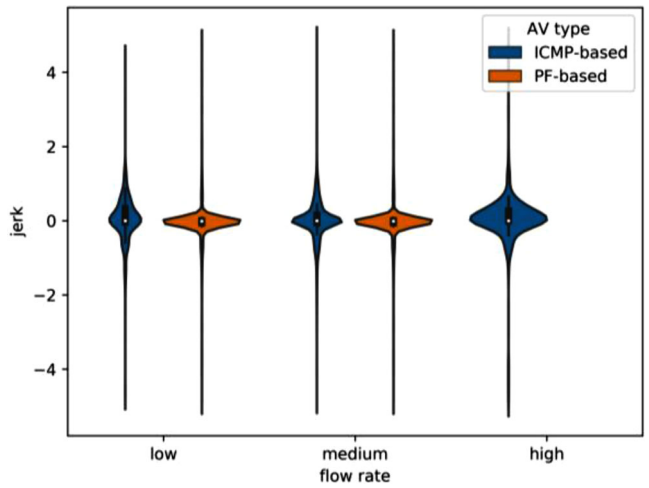

FIGURE 15 Jerks of two kinds of AVs with different oncoming flow rates

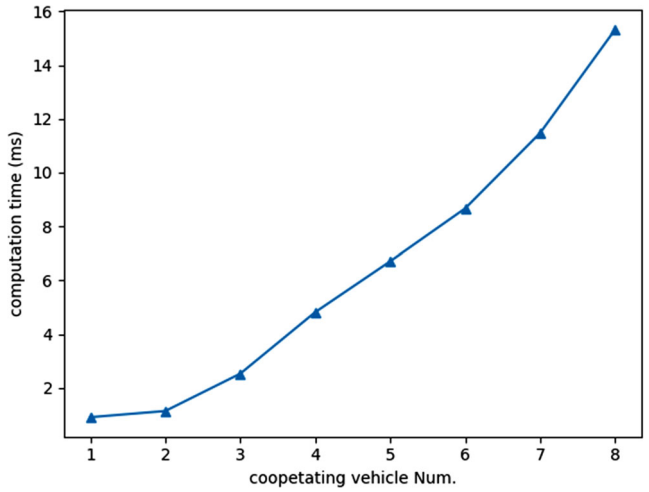

FIGURE 16 Computational time of the algorithm

than 1 m/s^3 , which meant that each type of vehicle performed well. The proposed ICMP method set a minimum-jerk based term in the object function for better driving smoothness, while the PF-based method set some constraints on acceleration. This is why the jerks of two AVs are insignificant. However, ICMP-based AVs had fewer instance of extreme jerk values. The reason was that the object function of speed planning aimed to minimize the sum of the jerk squared. Therefore, ICMP-based AVs tried to avoid sharp acceleration or deceleration.

5.4 | Computation time

The computational time (with Intel(R) Core(TM) i5-10210U CPU at 1.60 GHz 2.11 GHz) is shown in Figure 16. When interacting with multiple oncoming vehicles, the turn AV had to assume one vehicle as the cooperating object one by one and tried the ICMP to solve a planning until finding a solution. It means the computation time may be at most m times more than one motion planning, where m is the number of the oncoming vehicles. This issue may be relieved by more code optimization or distributed computing. However, we can just treat the leading five oncoming vehicles as the cooperating candidates so that the method can meet real-time computing requirement at 10-Hz update rate.

6 | CONCLUSION

Realizing the behavioural consistency is an essential but challenging issue for motion planning in multi-interaction environments. This paper proposed an ICMP framework that actively seeks the chance of cooperating with interacting participants. The main conclusions are summarized as follows:

1. Inspired by the process of behaviours asymptotically converging to consistency, the ICMP framework realized intended cooperation with interacting participants by predicting the response of the interacting participants to the AV's planning. By analyzing the interaction mechanism and instilling it in AV's planning, the ICMP achieved socially compliant driving which made it easier to arise cooperative response of the interacting participants. The cooperative acceleration-based criteria were learned from empirical analysis, and clearly indicated the response of the interacting participants to the turning vehicle's motion. By searching in the cooperative motion planning space derived from the criteria, feasible ICMP solutions were available. The ICMP reproduced the process of behaviours converging to consistency. The ICMP does not rely on a fixed intersection and so can be applicable in other intersections. Besides, it may be extended to other cooperation-involved scenarios like on-ramp merging bottlenecks.
2. A Gaussian mixture model was developed to learn the human drivers' preference for determining conflict points. First, since the prediction and the planning are interrelated, AVs would be trapped in the causal dilemma about which term should be handled first. The conflict points are the knots that link the response prediction and the path planning together, so rapidly determining conflict points can avoid this causal dilemma. In addition, it helped narrow down the solution spaces of planning by extracting conflict points with higher human drivers' preference.
3. Compared with PF-based AVs, ICMP-based AVs were significantly safer when suffering low and medium oncoming flow rate participants. In addition, ICMP-based AVs yielded less large travel-time trajectories because ICMP-based AVs were more active and had more motion planning space to improve their efficiency. Finally, ICMP-based AVs had better comfort performance as they performed less sharp braking or acceleration.

In the future, the cooperative interaction mechanism can be extended to other types of participants like non-motorized vehicles and pedestrians. However, since the intention of

non-motorized vehicles and pedestrians is more flexible and changeable, a single index like cooperative acceleration may not be sufficient to represent their intentions. More representative indices can be extracted based on more data sources. Furthermore, as the dimension of intention representation increases, mapping on the motion planning space may become non-linear or implicit. Machine learning methods can be applied to solve the problem. All these directions can be considered in further research.

ACKNOWLEDGEMENTS

This research was sponsored by the National Key Research and Development Program of China (2018YFB1600505) and the National Natural Science Foundation of China (52125208).

CONFLICTS OF INTEREST

The authors declare no conflicts of interests.

DATA AVAILABILITY STATEMENT

The data used to support the findings of this study are available from the corresponding author upon request.

ORCID

Donghao Zhou https://orcid.org/0000-0001-5708-3925
Xiaohui Zhang https://orcid.org/0000-0001-8613-076X
Jian Sun https://orcid.org/0000-0001-5031-4938

REFERENCES

1. National Highway Traffic Safety Administration.: Traffic Safety Facts: 2008 Data. Washington, DC: National Highway Traffic Safety Administration (2008).
2. Troutbeck, R.J., Kako, S.: Limited priority merge at unsignalized intersections. Transp. Res. A Policy Pract.33(3–4), 291-304 (1999). https://doi.org/10.1016/S0965-8564(98)00046-9
3. Alhajyaseen, W.K.M., Asano, M., Nakamura, H., Dang, M.T.: Stochastic approach for modeling the effects of intersection geometry on turning vehicle paths. Transp. Res. Part C Emerg. Technol.32, 179–192 (2013). https://doi.org/10.1016/j.trc.2012.09.006
4. Zhan, W., Liu, C., Chan, C.Y., Tomizuka, M.: A non-conservatively defensive strategy for urban autonomous driving. In: 2016 IEEE 19th International Conference on Intelligent Transportation Systems (ITSC) (2016).
5. Noh, S.: Decision-making framework for autonomous driving at road intersections: Safeguarding against collision, overly conservative behavior, and violation vehicles. IEEE Trans. Ind. Electron.66(4), 3275–3286 (2019). https://doi.org/10.1109/TIE.2018.2840530
6. D'Onfro, J.: 'I hate them': Locals reportedly are frustrated with Alphabet's self-driving cars. ed. CNBC, 2018, https://www.cnbc.com/2018/08/28/locals-reportedly-frustrated-with-alphabets-waymo-self-driving-cars.html.
7. Polychronopoulos, A., Tsogas, M., Amditis, A.J., Andreone, L.: Sensor fusion for predicting vehicles' path for collision avoidance systems. IEEE Trans. Intell. Transp. Syst.8(3), 549–562 (2007). https://doi.org/10.1109/TITS.2007.903439
8. Agamennoni, G., Nieto, J.I., Nebot, E.M.: Estimation of multivehicle dynamics by considering contextual information. IEEE Trans. Rob.28(4), 855–870 (2012). https://doi.org/10.1109/TRO.2012.2195829
9. Gindele, T., Brechtel, S., Dillmann, R.: Learning context sensitive behavior models from observations for predicting traffic situations. In: International IEEE Conference on Intelligent Transportation Systems, 2013, 1764–1771: IEEE.
10. Bahram, M., Lawitzky, A., Friedrichs, J., Aeberhard, M., Wollherr, D.: A game-theoretic approach to replanning-aware interactive scene prediction and planning. IEEE Trans. Veh. Technol.65(6), 3981–3992 (2015). https://doi.org/10.1109/TVT.2015.2508009
11. Wei, J., Dolan, J.M., Snider, J.M., Litkouhi, B.: A point-based mdp for robust single-lane autonomous driving behavior under uncertainties. In: IEEE International Conference on Robotics and Automation, 2011, 2586–2592.
12. Ong, S.C., Png, S.W., Hsu, D., Lee, W.S.: Planning under uncertainty for robotic tasks with mixed observability. Int. J. Robot. Res.29(8), 1053–1068 (2010). https://doi.org/10.1177/0278364910369861
13. Schwarting, W., Pierson, A., Alonso-Mora, J., Karaman, S., Rus, D.: Social behavior for autonomous vehicles. Proc. Natl. Acad. Sci.116(50), 24972–24978 (2019). https://doi.org/10.1073/pnas.1820676116
14. Ammoun, S., Nashashibi, F.: Real time trajectory prediction for collision risk estimation between vehicles. In: 2009 IEEE 5th International Conference on Intelligent Computer Communication and Processing, 2009, 417–422.
15. Xu, W., Pan, J., Wei, J., Dolan, J.M.: Motion planning under uncertainty for on-road autonomous driving. In: 2014 IEEE International Conference on Robotics and Automation (ICRA), 2014, 2507–2512.
16. Sun, J., Qi, X., Xu, Y., Tian, Y.: Vehicle turning behavior modeling at conflicting areas of mixed-flow intersections based on deep learning. IEEE Trans. Intell. Transp. Syst.21(9), 3674–3685 (2019). https://doi.org/10.1109/TITS.2019.2931701
17. Lenz, D., Diehl, F., Le, M.T., Knoll, A.: Deep neural networks for Markovian interactive scene prediction in highway scenarios. In: IEEE Intelligent Vehicles Symposium (2017).
18. Chen, Z., Ngai, D.C., Yung, N.: Pedestrian behavior prediction based on motion patterns for vehicle-to-pedestrian collision avoidance. In: 2008 11th International IEEE Conference on Intelligent Transportation Systems, 316–321 (2008).
19. Ma, Z., Sun, J., Wang, Y.: A two-dimensional simulation model for modelling turning vehicles at mixed-flow intersections. Transp. Res. Part C Emerg.75, 103–119 (2017). https://doi.org/10.1016/j.trc.2016.12.005
20. Ma, Z., Xie, J., Qi, X., Xu, Y., Sun, J.: Two-dimensional simulation of turning behavior in potential conflict area of mixed-flow intersections. Comput.-Aided Civ. Infrastruct. Eng.32(5), 412–428 (2017). https://doi.org/10.1111/mice.12266
21. Xu, Y., Ma, Z., Sun, J.: Simulation of turning vehicles' behaviors at mixed-flow intersections based on potential field theory. Transportmetrica B: Transport Dynamics7(1), 498–518 (2019). https://doi.org/10.1080/21680566.2018.1447407
22. Chen, Q., Ozguner, U., Redmill, K.: Ohio State University at the 2004 DARPA grand challenge: Developing a completely autonomous vehicle. IEEE Intell. Syst.19(5), 8–11 (2004). https://doi.org/10.1109/MIS.2004.48
23. Thrun, S., et al.: Stanley: The robot that won the DARPA Grand Challenge. J. Field Rob.23(9), 661–692 (2006). https://doi.org/10.1002/rob.20147
24. Yoo, J., Langari, R.: A predictive perception model and control strategy for collision-free autonomous driving. IEEE Trans. Intell. Transp. Syst.20, 4078–4091 (2019). https://doi.org/10.1109/TITS.2018.2880409
25. Rahmati, Y., Hosseini, M.K., Talebpour, A.: Helping automated vehicles with left-turn maneuvers: A game theory-based decision framework for conflicting maneuvers at intersections. IEEE Trans. Intell. Transp. Syst.1–14 (2021). https://doi.org/10.1109/TITS.2021.3108409
26. Tran, Q., Firl, J.: Online maneuver recognition and multimodal trajectory prediction for intersection assistance using non-parametric regression. In IEEE Intelligent Vehicles Symposium Proceedings, 918–923 (2014).
27. Shu, H., Liu, T., Mu, X., Cao, D.: Driving tasks transfer using deep reinforcement learning for decision-making of autonomous vehicles in unsignalized intersection. IEEE Trans. Veh. Technol.71, 41–52, (2021). https://doi.org/10.1109/TVT.2021.3121985
28. Yao, R., Zeng, W., Chen, Y., He, Z.: A deep learning framework for modelling left-turning vehicle behaviour considering diagonal-crossing motorcycle conflicts at mixed-flow intersections. Transp. Res. Part C Emerg. Technol.132, 103415 (2021). https://doi.org/10.1016/j.trc.2021.103415
29. Shu, K., et al.: Autonomous driving at intersections: A critical-turning-point approach for left turns. arXiv preprint arXiv02409 (2020).

30. Hubmann, C., Schulz, J., Becker, M., Althoff, D., Stiller, C.: Automated driving in uncertain environments: Planning with interaction and uncertain maneuver prediction. IEEE Trans. Intell. Veh.3, 5–17, (2018). https://doi.org/10.1109/TIV.2017.2788208
31. Shu, K., et al.: Autonomous driving at intersections: A behavior-oriented critical-turning-point approach for decision making. IEEE/ASME Trans. Mechatron.27, 234–244, (2021). https://doi.org/10.1109/TMECH.2021.3061772
32. Gindele, T., Brechtel, S., Dillmann, R.: Learning driver behavior models from traffic observations for decision making and planning. IEEE Intell. Transp. Syst. Mag.7(1), 69–79 (2015). https://doi.org/10.1109/MITS.2014.2357038
33. Brechtel, S., Gindele, T., Dillmann, R.: Probabilistic decision-making under uncertainty for autonomous driving using continuous POMDPs. In: IEEE International Conference on Intelligent Transportation Systems (2014).
34. Trautman, P., Ma, J., Murray, R.M., Krause, A.: Robot navigation in dense human crowds: Statistical models and experimental studies of human–robot cooperation. Int. J. Robot. Res.34, 335–356, (2015). https://doi.org/10.1177/0278364914557874
35. Aghili, F.: A prediction and motion-planning scheme for visually guided robotic capturing of free-floating tumbling objects with uncertain dynamics. IEEE Trans. Rob.28(3), 634–649 (2012). https://doi.org/10.1109/TRO.2011.2179581
36. Ferguson, D., Darms, M., Urmson, C., Kolski, S.: Detection, prediction, and avoidance of dynamic obstacles in urban environments. In: 2008 IEEE Intelligent Vehicles Symposium, 2008, 1149–1154.
37. Woo, H., et al.: Lane-change detection based on vehicle-trajectory prediction. IEEE Robot. Atom. Lett. 2(2), 1109–1116 (2017).
38. Kuwata, Y., Teo, J., Karaman, S., Fiore, G., Frazzoli, E., How, J.: Motion planning in complex environments using closed-loop prediction. In: AIAA Guidance, Navigation and Control Conference and Exhibit, 7166 (2008).
39. Gadepally, V., Krishnamurthy, A., Ozguner, U.: A framework for estimating driver decisions near intersections. IEEE Trans. Intell. Transp. Syst.15(2), 637–646 (2013). https://doi.org/10.1109/TITS.2013.2285159
40. Hülnhagen, T., Dengler, I., Tamke, A., Dang, T., Breuel, G.: Maneuver recognition using probabilistic finite-state machines and fuzzy logic. In: IEEE Intelligent Vehicles Symposium, 65–70 (2010).
41. Gu, Y., Hashimoto, Y., Hsu, L.-T., Iryo-Asano, M., Kamijo, S.: Human-like motion planning model for driving in signalized intersections. IATSS Res.41, 129 (2017). https://doi.org/10.1016/j.iatssr.2016.11.002
42. Schlechtriemen, J., Wedel, A., Breuel, G., Kuhnert, K.D.: A probabilistic long term prediction approach for highway scenarios. In: IEEE 17th International Conference on Intelligent Transportation Systems (ITSC) (2014).
43. Chen, C., He, Y.Q., Bu, C.G., Han, J.D., Zhang, X.: Quartic Bezier curve based trajectory generation for autonomous vehicles with curvature and velocity constraints. In: IEEE International Conference on Robotics & Automation (2014).
44. Takahashi, A., Hongo, T., Ninomiya, Y., Sugimoto, G.: Local path planning and motion control for agv in positioning. In: IEEE/RSJ International Workshop on Intelligent Robots and Systems'.(IROS'89)'The Autonomous Mobile Robots and Its Applications. 392–397 (1989).
45. Liebner, M., Klanner, F., Baumann, M., Ruhhammer, C., Stiller, C.: Velocity-based driver intent inference at urban intersections in the presence of preceding vehicles. IEEE Intell. Transp. Syst. Mag.5(2), 10–21 (2013). https://doi.org/10.1109/MITS.2013.2246291
46. Zhou, D., Ma, Z., Sun, J.: Autonomous vehicles' turning motion planning in multi-interaction area of mixed-flow intersections. IEEE Trans. Intell. Vehicles5, 204–216 (2019). https://doi.org/10.1109/TIV.2019.2955854
47. Ismail, K., Sayed, T., Saunier, N.: Methodologies for aggregating indicators of traffic conflict. Transp. Res. Rec.2237, 10–19 (2011). https://doi.org/10.3141/2237-02

How to cite this article: Zhou, D., Ma, Z., Zhang, X., Sun, J.: Autonomous vehicles' intended cooperative motion planning for unprotected turning at intersections. IET Intell. Transp. Syst. 16, 1058–1073 (2022). https://doi.org/10.1049/itr2.12195

APPENDIX

The Proof of Two Claims

We first prove **Claim 1**.

Since feasible solutions to the AV's motion planning exist among the cooperating time range T_p , then

$$T_l \le T_p \tag{A.1}$$

where T_l is the time to the conflict point for the left-turning AV.

According to the definition of the cooperative acceleration, there is

$$T_s = T_l \tag{A.2}$$

So

$$T_s \le T_p \tag{A.3}$$

where T_s is the time to the conflict point for the cooperating participant.

According to Equations (1) and (2), we know

$$\begin{aligned} v_s\left(T_p - T_s\right) + \frac{1}{2}\left(H{T_p}^2 - a_c{T_s}^2\right) &= 0 \\ v_s\left(T_p - T_s\right) + \frac{1}{2}\left(H{T_p}^2 - a_c{T_s}^2\right) &= 0 \end{aligned} \tag{A.4}$$

Since $T_s \le T_p$, then

$$H{T_p}^2 \le a_c{T_s}^2 \tag{A.5}$$

Then we can get

$$H \le a_c\frac{{T_s}^2}{{T_p}^2} < a_c \tag{A.6}$$

According to the criteria for cooperative response, the cooperative acceleration being large than H indicates that the interacting agent is willing to yield to the AV.

The proof of **Claim 2** can be acquired by replacing ' $\le$ ' and ' $<$ ' with ' $\ge$ ' and ' $>$ ' in the proof of **Claim 1** so it is omitted here.